

Sn RADIOACTIVITY OF LANTHANIDE NUCLEI USING SKYRME ENERGY DENSITY FORMALISM*

GUDVEEN SAWHNEY^a, RAJNI^b, AJAY KUMAR RAI^b
MANOJ K. SHARMA^a

^aDepartment of Physics and Materials Science
Thapar Institute of Engineering and Technology
Patiala 147004, Punjab, India

^bDepartment of Physics
Sardar Vallabhbhai National Institute of Technology
Surat 395007, Gujarat, India

*Received 27 October 2023, accepted 17 January 2024,
published online 24 April 2024*

In this paper, we conducted a scientific exploration of cluster radioactivity, with a specific focus on lanthanide parents such as $^{120-124}\text{Ce}$, $^{124-128}\text{Sm}$, and $^{130-134}\text{Gd}$ originating from the trans-tin region. The primary objective of this study is to gain insights into the fragmentation and structural characteristics of these nuclei. To achieve this, we have employed Skyrme Energy Density Formalism (SEDF) within the framework of the Preformed Cluster Model (PCM). This model addresses the cluster emission process, which involves tunneling through a potential barrier, with the fragments preformed and having a relative probability denoted as P_0 . Our investigation highlights the influence of deformation and orientation effects on potential energy surfaces, preformation probability, barrier penetrability, and decay half-life, shedding light on the crucial role of nuclear shape and structure in view of cluster radioactivity.

DOI:10.5506/APhysPolBSupp.17.3-A29

1. Introduction

The concept of cluster radioactivity has gained validation in both experimental [1] and theoretical [2] aspects, in addition to the more common emissions such as α , β , and γ radiation. A complete range of these decay processes, encompassing clusters from light to heavy (^{14}C to ^{34}Si) has been identified originating from a number of actinide elements ranging from ^{221}Fr to ^{242}Cm . Nonetheless, efforts to explore additional cluster emissions

* Presented at the XXXVII Mazurian Lakes Conference on Physics, Piaski, Poland, 3–9 September, 2023.

are actively in progress. Having an understanding of shell effects in the region beyond lead (Pb) on the periodic table, it was anticipated [3] that the trans-tin region could also be a favorable zone for the possible occurrence of cluster radioactivity. In this context, the involvement of closed-shell daughter nuclei such as ^{100}Sn or ^{132}Sn , along with their adjacent isotopes, might enhance the probability of cluster emission. To explore this region, ground state ($T = 0$) decays of $^{108-116}\text{Xe}$, $^{112-120,146}\text{Ba}$, $^{116-124,152}\text{Ce}$, $^{120-130,156}\text{Nd}$, $^{124-130,160,162}\text{Sm}$, and $^{128-136,166}\text{Gd}$ nuclei have been analyzed in [4]. It has been observed [4] that while neutron-rich radioactive nuclei decay by emitting clusters via a non-alpha-like structure, $A_2 = 4n + 2$, regardless of the choice of spherical or deformed fragmentation, neutron-deficient parents emit with an alpha-like structure ($A_2 = 4n$) cluster along with doubly magic ^{100}Sn , where n refers to the number of nucleons in the fragment. This study is conducted with a preformed cluster model (PCM) [4–7], in which clusters of different sizes are preformed in the parent nucleus with relative formation probability in relation to remaining fragments in the binary exit channel.

Motivated by the above analysis [4], in the present work, we intend to investigate the ground state of even isotopes of lanthanide parents $^{120-124}\text{Ce}$, $^{124-128}\text{Sm}$, and $^{130-134}\text{Gd}$ using the Skyrme energy density formalism (SEDF) [8, 9]. It may be noted that the Blocki-based nuclear potential was employed in the previously published work [4], however the density-based formalism (SEDF) [8, 9] is used in the current study. Another motivation for the present work is based on our recent study [6] where we examined the cluster decay within the trans-lead region such as Ra, Th, U, and Pu nuclei referring to lead or neighboring nuclei as a daughter product. The selected Skyrme forces (SIII, SkI4, and SAMi) yielded reasonable predictions [6] for the observed cluster decay, with SIII [10] performing substantially better for nuclei of heavier mass. In view of this, the aim of the present work is to analyze the influence of a density-dependent potential (SIII force) within the framework of PCM on the behavior of possible fragmentation of Ce, Sm, and Gd parents. Here, we intend to analyze the behaviour of potential energy surfaces (PES) along with half-life to explore the possible role of shell closure effects. Considering the crucial role played by the shape of the nucleus, the explicit role of deformation and orientations is studied by comparing the results with the spherical case. It may be noted that deformation effects up to quadrupole β_2 are included within the “optimum” orientation [11] approach. Knowing that the PCM handles the fragmentation process through a collective approach of clustering, it is fascinating to investigate how the deformation and orientation effects of the decay fragments impact the interaction potential and, consequently, the PES of these lanthanide nuclei.

2. Methodology

Derived from the quantum mechanical fragmentation theory (QMFT), the Preformed Cluster Model (PCM) [4–7] is formulated using collective parameters encompassing the mass (η_A) and charge (η_Z) asymmetries along-with the relative separation (R), the multipole deformations $\beta_{\lambda i}$ ($\lambda = 2, 3, 4$; $i = 1, 2$), and orientations θ_i of decaying (heavy and light) fragments. The decay constant λ or decay half-life time $T_{1/2}$ in PCM is defined as

$$T_{1/2} = \frac{\ln 2}{\lambda}, \quad \lambda = \nu_0 P_0 P. \quad (1)$$

Here, P_0 represents the preformation probability of the disintegrating fragments, while P signifies the barrier penetrability, referring to η and R -motions, respectively. ν_0 ($\sim 10^{21} \text{ s}^{-1}$) is the barrier assault frequency of the preformed cluster.

The structure information of the decaying nucleus is contained in P_0 via the fragmentation potential V and is defined as

$$\begin{aligned} V = & - \sum_{i=1}^2 [B_i(A_i, Z_i)] + V_C(R_i, Z_i, \beta_{\lambda i}, \theta_i) \\ & + V_N(R_i, A_i, \beta_{\lambda i}, \theta_i) + V_\ell(R_i, A_i, \beta_{\lambda i}, \theta_i). \end{aligned} \quad (2)$$

V_C , V_N , and V_ℓ are, respectively, the Coulomb, nuclear, and angular momentum-dependent potentials for deformed and oriented nuclei (for details, refer to Ref. [5]). Here, $B_i(A_i, Z_i)$ are the ground-state binding energies taken from references [12, 13].

The radius vector $R_i(\alpha_i)$ ($i = 1, 2$), through which deformation and orientation effects are added, is defined as

$$R_i(\alpha_i, T) = R_{0i}(T) \left[1 + \sum_{\lambda} \beta_{\lambda i} Y_{\lambda}^{(0)}(\alpha_i) \right] \quad (3)$$

with half-density radii R_{0i} given by [14] as

$$\begin{aligned} R_{0i}(T = 0) = & 0.9543 + 0.0994 A_i - 9.8851 \times 10^{-4} A_i^2 \\ & + 4.8399 \times 10^{-6} A_i^3 - 8.4366 \times 10^{-9} A_i^4. \end{aligned} \quad (4)$$

Here, $Y_{\lambda}^{(0)}(\alpha_i)$ are the spherical harmonic functions and α_i is an angle formed by the radius vector R_i with the symmetry axis, measured clockwise [11]. In the present work, quadrupole deformations (β_{2i} ; $i = 1, 2$ for cluster and daughter respectively) of decaying fragments are considered.

In Eq. (2), the nuclear potential V_N between two colliding nuclei is calculated within the framework of the Skyrme energy density formalism [8, 9] as

$$V_N(R) = E_{\text{tot}}(R) - E_1 - E_2, \quad (5)$$

where

$$E_{\text{tot}}(R) = \int H[\rho_p(\vec{r}), \rho_n(\vec{r})] d\vec{r}, \quad (6)$$

$$E_i(R) = \int H[\rho_{ip}(\vec{r}), \rho_{in}(\vec{r})] d\vec{r}, \quad (i = 1, 2). \quad (7)$$

Here, $E_{\text{tot}}(R)$ is the total energy expectation value of the colliding partners at distance R (center to center), whereas the individual energies of non-interacting projectile and target nuclei are represented by E_1 and E_2 . Here, $\rho_{ip}(r)$, $\rho_{in}(r)$ are proton and neutron densities of non-interacting nuclei and $\rho_p(r)$, $\rho_n(r)$ densities of interacting nuclei. $H(r)$ in the above equation stands for energy density functional given as in [8], including the kinetic energy contribution $\tau(r)$ and nuclear interaction parts $H_{\text{sky}}(r)$.

3. Calculations and results

With an aim to explore the structural characteristics, Fig. 1 illustrates the fragmentation potential as a function of cluster mass for the considered ^{122}Ce , ^{124}Sm , and ^{132}Gd parents. A comparison is conducted for both spherical and β_2 -deformed fragment choices, aiming to understand the properties of these radioactive nuclei within the trans-Sn region. It is important to note that our focus is solely on potential energy minima because the corresponding preformation factor P_0 is maximized compared to neighboring fragments. The minima in the fragmentation potential predominantly arise due to the shell closure effects (spherical or deformed) of one or both fragments, providing insights into nuclear structure effects. Three key findings are evident from Fig. 1: (i) While there are variations in the magnitude of the fragmentation potential, the structures of PES exhibit similarity regardless of spherical or deformed fragments; (ii) The status of the favorable cluster remains intact, independent of the shape of fragments; (iii) The preferred clusters shift toward the heavier mass region with the increase in mass number of parent nuclei. Apparently, the most favorable clusters in the decay of ^{122}Ce , ^{124}Sm and ^{132}Gd parents are ^{16}O , ^{24}Mg , and ^{28}Si , respectively, which indicates their likely occurrence along with their corresponding daughters such as ^{106}Sn , ^{100}Sn , and ^{104}Sn .

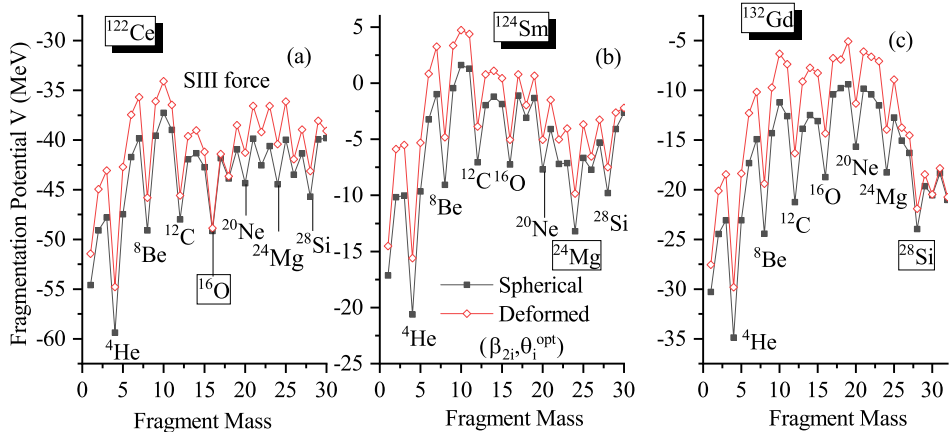


Fig. 1. PCM calculated fragmentation potentials for the decay of (a) ^{122}Ce , (b) ^{124}Sm , and (c) ^{132}Gd considering spherical and β_2 deformed choice of decaying fragments.

It is worth mentioning that when the fragmentation potential depicted in Fig. 1 is normalized relative to the binding energy, it provides the scattering potential which is used to compute the barrier penetrability P . Here, P is calculated by solving the WKB integral between the R_a and R_b , the

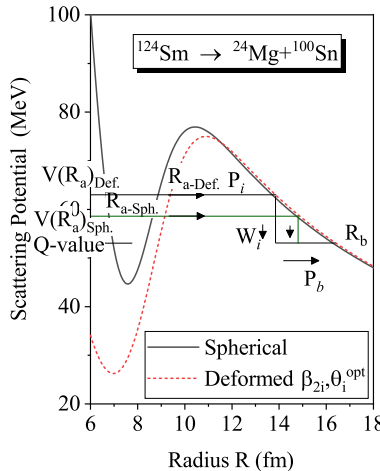


Fig. 2. Scattering potentials for the spontaneous decay of $^{124}\text{Sm} \rightarrow ^{24}\text{Mg} + ^{100}\text{Sn}$, showing the three steps of barrier penetration used in PCM: (i) the penetrability P_i from R_a to R_i , (ii) the (inner) de-excitation probability W_i at R_i , taken as unity, i.e., $W_i = 1$ for heavy cluster decays [15], and (iii) the penetrability P_b from R_i to R_b . Here, $V(R_a)$ represents the value of potential at the first tunneling point.

first and second turning points, respectively. Figure 2 shows a substantial impact on the scattering potential when transitioning from a spherical to a deformed configuration. This transition leads to significant changes in both barrier height and position, thereby influencing the tunneling probability. The calculated decay half-life ($T_{1/2}$) in PCM is reliant on penetrability (P) as per Eq. (1), and consequently, the choice of configuration significantly affects it. This observation implies the importance of selecting a spherical or deformed approach in investigating the half-lives and hence the decay of a particular nuclear system.

To explore further, Fig. 3 shows the computed preformation probabilities, penetrabilities, and logarithms of half-life times for the entire range of lanthanide parents considered, encompassing $^{120-124}\text{Ce}$, $^{124-128}\text{Sm}$, and $^{130-134}\text{Gd}$. Specifically, the calculations pertain to the clusters ^{16}O , ^{24}Mg , and ^{28}Si decaying individually from the isotopes of Ce, Sm, and Gd nuclei. For the majority of the parents investigated, we observe that both P_0 and P increase as one goes from spherical to deformed choice of shapes, highlighting the indispensable role of deformation effects. The resulting values of $\log_{10} T_{1/2}$ stemming from these factors are plotted in Fig. 3 (c). As expected, the magnitude of $\log_{10} T_{1/2}$ is observed to be least for the deformed configuration, varying widely from ~ 2 to 23, thereby presenting an interesting case of investigation. Note that our PCM-predicted half-lives fall within the experimental limits and align with earlier findings [3, 16, 17] derived from various mass tables. Such a study emphasizes the significance of deformation effects in determining the clusterization process and thus may serve as a testing ground for the future experiments on cluster decay studies in the trans-tin region.

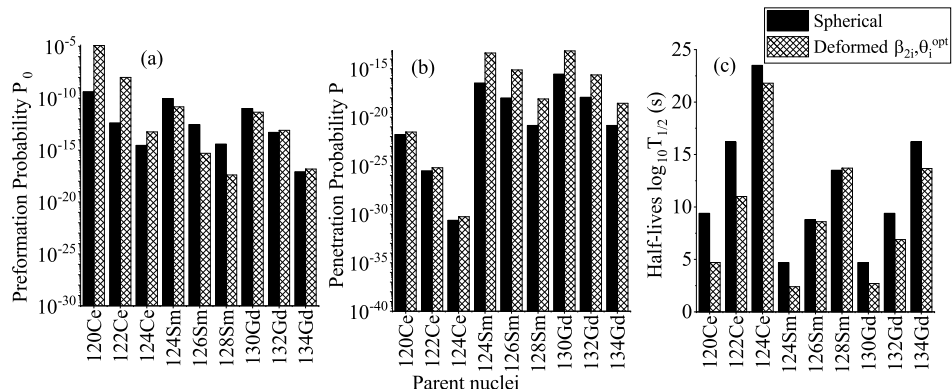


Fig. 3. Histogram representation of (a) preformation probability, (b) penetrability, and (c) logarithm of decay half-lives for the ^{16}O , ^{24}Mg , and ^{28}Si clusters emitted respectively from Ce, Sm, and Gd isotopes.

4. Summary and conclusions

To summarize, we have conducted a comprehensive investigation of the ground-state emission of $^{120-124}\text{Ce}$, $^{124-128}\text{Sm}$, and $^{130-134}\text{Gd}$ nuclei by employing the Preformed Cluster Model (PCM). We have investigated the specific influence of deformation and orientations by comparing the outcomes with the spherical scenario. By introducing deformation and orientation effects, we observed substantial modifications to the fragmentation potential, the penetration pathway, and the associated barrier characteristics. These modifications had a notable impact on both the preformation probability (P_0) and the penetrability (P) of the emitting cluster(s). The calculations are done by using SIII Skyrme force, which imparts an advantage to segregate spin-saturated and spin-dependent part of nuclear potential.

G.S. acknowledges the Department of Science and Technology, the Government of India for financial support vide reference No. “DST/WOS-A/PM-53/2021” under the Women Scientists Scheme A. Rajni is thankful to the Council of Scientific and Industrial Research (CSIR), New Delhi (File No. 09/1007(13391)/2022-EMR-I). M.K.S. is thankful for financial support from DST-SERB (grants No. CRG/2021/001144 and ITS/2023/003188) and PDA (TIET) to carry out this work.

REFERENCES

- [1] H.J. Rose, G.A. Jones, *Nature (London)* **307**, 245 (1984).
- [2] A. Săndulescu *et al.*, *Sov. J. Part. Nucl.* **11**, 6 (1980).
- [3] S. Kumar *et al.*, *Phys. Rev. C* **51**, 1762 (1995).
- [4] K. Sharma *et al.*, *Eur. Phys. J. A* **55**, 30 (2019).
- [5] G. Sawhney *et al.*, *Phys. Rev. C* **83**, 064610 (2011).
- [6] Rajni *et al.*, *Phys. Rev. C* **106**, 044605 (2022).
- [7] G. Sawhney *et al.*, *Eur. Phys. J. A* **50**, 175 (2014).
- [8] D. Vautherin, D.M. Brink, *Phys. Rev. C* **5**, 626 (1972).
- [9] Rajni *et al.*, *Eur. Phys. J. A* **53**, 208 (2017).
- [10] J. Friedrich, P.-G. Reinhard, *Phys. Rev. C* **33**, 335 (1986).
- [11] R.K. Gupta *et al.*, *J. Phys. G: Nucl. Part. Phys.* **31**, 631 (2005).
- [12] P. Möller *et al.*, *At. Data Nucl. Data Tables* **59**, 185 (1995).
- [13] G. Audi *et al.*, *Nucl. Phys. A* **729**, 337 (2003).
- [14] H. de Vries *et al.*, *At. Data Nucl. Data Tables* **36**, 495 (1987).
- [15] M. Greiner, W. Scheid, *J. Phys. G: Nucl. Phys.* **12**, L229 (1986).
- [16] D.N. Poenaru *et al.*, *Phys. Rev. C* **47**, 2030 (1993).
- [17] K.P. Santosh, *Pramana J. Phys.* **76**, 431 (2011).